Noise Coupling Mechanism Analysis and Mitigation Method for Receiver Sensitivity Improvement in an Optical QSFP Transceiver Module

Yuandong Guo[1#], Shuai Jin[2#], Xinglin Sun[3*], and Jun Fan[4#]
[#]Electromagnetic Compatibility Laboratory
Missouri University of Science and Technology
Rolla, Missouri, USA
[1]ydggdd, [2]sjfx7, [4]jfan@mst.edu
[*]College of Biomedical Engineering & Instrument Science
Zhejiang University
Hangzhou, China
[3]xlsun@zju.edu.cn

***Abstract*—The increasingly growth of the traffic in data centers demands for high-speed data transition and high bandwidth density. Optical communication is a promising way for the propagation of high-speed signals with less distortions. The quad small form-factor pluggable (QSFP) transceiver module is an essential component converting an electrical signal into an optical signal for point-to-point data transition. Considerable attentions have been paid to the signal integrity (SI) optimization for the optical QSFP transceiver modules with different data rates, where the receiver sensitivity is generally considered to be critical. In this paper, the receiver sensitivity problem of a typical QSFP transceiver module with 10 Gbit/s data rate is studied. It is the first time to demonstrate that the receiver sensitivity improvement is not only related with the SI design, but also connected with the electromagnetic interference (EMI) mitigation inside the DUT. The convential simulation model used for SI analysis with important metal configurations excluded is limited in the ability to identify the coupling between the radiating structures. It is found that the EMI noise induced by the unbalanced PCB routing and the interconnect between the PCB and flexible printed circuit (FPC) has significant contribution to the total noise at the receiver end. The generation of the antenna-mode current is verified and further studied using the full wave simulations. The mitigation method is proposed and confirmed through the measurements to improve the receiver sensitivity.**

Keywords—optical transceiver module, electromagnetic interference, antenna-mode current, common mode, mode conversion, imbalance difference model, crosstalk, transmission line, differential mode.

I. INTRODUCTION

The continuous increase of the traffic in the data centers requires high data rate and bandwidth density. Optical communication has become a promising way to propagate high-speed signals with limited distortions [1]. The quad small form-factor pluggable (QSFP) transceiver module used in the data centers and servers is an important component which converts an electrical signal into an optical signal for the point-to-point high-speed transition. Considerable attentions have been paid in the past to the signal integrity (SI) issues of the optical QSFP transceiver modules with various data rates and configurations [2]-[7]. The receiver sensitivity is generally considered to be critical in the high-speed applications where the optical QSFP transceiver modules are involved.

The crosstalk between the receiver and adjacent PCB channels is a crucial concern in the SI design and optimization due to the limited space, the nature of the PCB transmission lines of an optical QSFP transceiver module, and the continuous increase of the data rate. Excessively electromagnetic crosstalk noise may cause the degradation of receiver sensitivity [8], [9]. The analysis for crosstalk reduction aiming for the improvement of receiver sensitivity for optical QSFP transceiver modules have been conducted in [10]-[15] with the focus on the passive coupling between the aggressive and victim channels. A comprehensive perspective on far-end crosstalk (FEXT) form factors for transmission lines with mismatched terminals is proposed in [16].

The optical QSFP transceiver modules are typically mounted at the front-end of a system. Electromagnetic interference (EMI) problems may occur due to the high frequency of the components inside the optical transceiver modules and the mounting configurations on the metal chassis [17], [18]. The EMI coupling paths and various mitigation methods are proposed in [19]-[21]. However, these studies concentrate on the system-level or component-level EMI issues and ignore the EMI noise inside an optical QSFP transceiver module which may result in receiver sensitivity degradation.

In this paper, the receiver sensitivity problem of an optical QSFP transceiver module with 10 Gbit/s data rate is studied. It is the first time to demonstrate that the receiver sensitivity improvement is not only related with the SI design of the product, but also connected with the EMI noise cancellation inside the optical transceiver module under study. The complete structure of the DUT needs to be considered in the analysis to include the coupling between the radiators. It is found that the EMI noise inside the DUT has significant contribution to the total noise level at the receiver end.

The unwanted radiated emissions caused by the unintended common-mode (CM) currents present a challenging EMI problem [22]. The imbalance difference model introduced in [22]-[24] is adopted in this paper to explain and analyze the antenna-mode (AM) noise generation mechanism. In the model, the AM propagation is defined as a special situation of the CM propagation, where the currents on both signal and reference conductors flow toward the same

direction. It is shown that the CM current induced by the imbalances in the PCB traces becomes AM current resulted from the differences in the imbalance factors of the transmission lines on both PCB and FPC, which generates excessive electromagnetic noise and degrade the receiver sensitivity of the DUT.

The noise coupling mechanism and generation of the AM current is first analyzed and identified in Section III after a brief introduction to the optical QSFP transceiver module and the crosstalk noise suppression in Section II. Simulation-based analysis is performed and demonstrated in Section IV to describe the impact of the EMI noise induced by the AM current on the receiver sensitivity quantitatively and qualitatively. The mitigation method is proposed and experimentally verified in Section V.

II. The Optical QSFP Transceiver Module and Receiver Sensitivity Issue

A. The Optical QSFP Transceiver Module

The block diagram of the optical QSFP transceiver module under study is shown in Fig. 1, comprising a bi-directional optical sub assembly (BOSA), FPCs for both transmitter (TX) and receiver (RX) channels, and a 10-layer PCB mounted with a Driver IC and a MCU. All the components are integrated into a metal chassis indicated by the black dotted box in Fig. 1. The data rate is 10 Gbit/s.

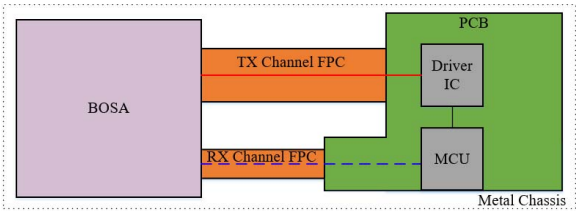

Fig. 1. The configuration of the optical QSFP transceiver module under study.

B. The Crosstalk Noise Suppression and Receiver Sensitivity Issue

It was found that there was a closed "eye" in the eye diagram measured at the receiver side due to the poor receiver sensitivity under the initial design, where the TX and RX channels were routed on the top and bottom layers separately using microstrip-lines on both PCB and FPCs for crosstalk noise suppression as illustrated in Fig. 1.

To further reduce the crosstalk level, the guarding traces have been employed on the FPCs for both TX and RX channels as can be observed in the full wave model exhibited in Fig. 2, where only the PCB and FPCs are included. The simulated magnitude of the FEXT at port 2 is demonstrated in Fig. 3, where it is found that the maximum magnitude of FEXT over the entire frequency range of interest is under -40 dB. However, the "eye" remains closed in the eye diagram implying that the improvement on the receiver sensitivity is limited if only lowering down the passive coupling between the channels.

III. Indentification of Noise Coupling Mechanism and the Generation of Antenna-mode Current

The PCB transmission lines of the TX channel is sketched in Fig. 4. The differential signal coming out from the Driver

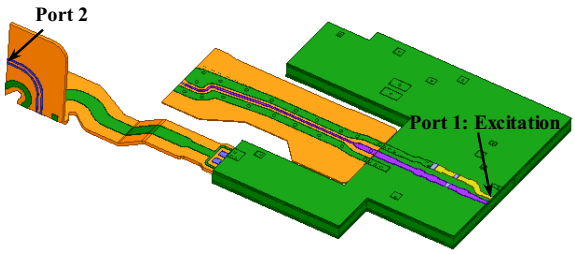

Fig. 2. The full wave model for crosstalk simulation with only PCB and FPCs included.

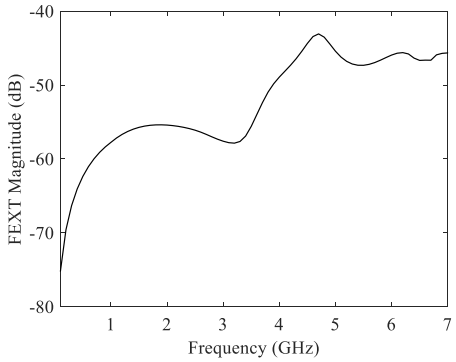

Fig. 3. The simulated FEXT magnitude at the receiver end with the guarding traces on both TX and RX channels.

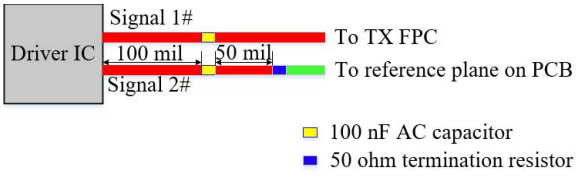

Fig. 4. Demonstration of the PCB routing of the TX channel.

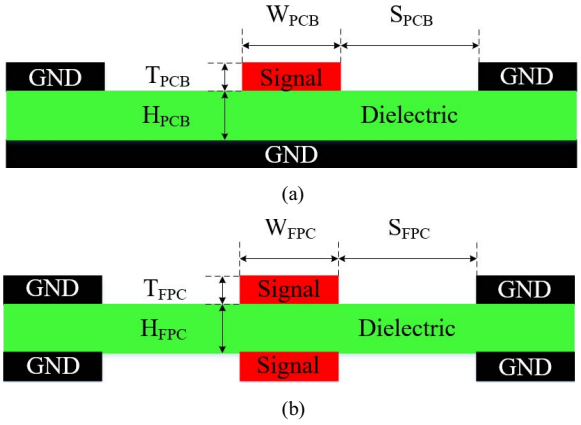

Fig. 5. Cross-sections of the PCB and FPC transmission lines at their interface for the TX channel: (a) PCB transmission line, (b) FPC transmission line.

IC starts to propagate on a single-ended trace with the other trace terminated by a 50 *ohm* resistor. This design introduces significant imbalances to the overall circuit network between the Drive IC and BOSA, which may cause CM noise propagating on the PCB converted from the differential-mode signal.

The cross-sections of the PCB and FPC transmission lines for the TX channel at their interface are illustrated in Fig. 5. The two signal conductors in Fig. 5 (b) are connected through

vias and merger together after 45 mil from the interface to form a single-ended transmission line on the FPC. The values of all geometrical parameters are given in Table I.

TABLE I. VALUES OF THE GEOMETRIES IN FIG. 5

Para.	Value	Para.	Value
W_{PCB}	18.0 mil	W_{FPC}	16.0 mil
S_{PCB}	13.0 mil	S_{FPC}	14.0 mil
T_{PCB}	1.2 mil	T_{FPC}	0.7 mil
H_{PCB}	3.0 mil	H_{FPC}	2.0 mil

For a given cross-section of a microstrip-line, the imbalance factor can be calculated using [24]

$$h = \frac{C_{trace}}{C_{trace} + C_{GND}} \tag{1}$$

where C_{trace} and C_{GND} are the per-unit-length stray capacitances of the signal trace and reference conductor, respectively. The 2D electrostatic solver, QuickField Students' version, is adopted in this study to compute the stray capacitances based on the cross-sectional geometries. The simulation results and the calculated imbalance factors for the PCB and FPC transmission lines are shown in Table II.

The difference in the imbalance factors is $h_{FPC} - h_{PCB} = 0.1008$, which results in the conversion of CM current to AM current, causing the radiated emission inside the DUT. The magnitude of the AM current is calculated with the help of full wave simulations and demonstrated in Section IV.

As aforementioned, AM current flows on both the signal and reference conductors. Inside the DUT, the reference planes of the PCB and FPCs are connected to the metal surface of the BOSA. Thus, the EMI current is propagating from the PCB to the BOSA through the TX FPC, which enables a radiating structure that can be observed in Fig. 6 where a full wave model representing the entire DUT is demonstrated. The metal chassis is intentionally not illustrated for better demonstration of the DUT.

Similarly, it can be expected that the PCB, RX FPC, and BOSA surface construct another radiator inside the DUT. Therefore, besides the passive coupling between the aggressive and victim channels, the coupling noise between the two radiating structures also contributes to the total noise level at the receiver end.

The limitations of the conventional SI analysis is also revealed which is based on the simplified full wave simulation model illustrated in Fig. 2, where the BOSA is not included indicating that the simulation is done without accounting for the complete structure of the DUT and the coupling between the radiators.

IV. SIMULATION-BASED ANALYSIS OF THE IMPACT OF EMI NOISE ON RECEIVER SENSITIVITY

To describe the influence of the EMI noise on DUT's receiver sensitivity quantitatively and qualitatively, a full wave model with only PCB excluded is built in ANSYS HFSS and presented in Fig. 7.

TABLE II.

SUMMARY OF THE SIMULATED STRAY CAPACITANCES AND CALCULATED IMBALANCE FACTORS

Para.	Value	Para.	Value
C_{trace_PCB}	0.9 pF/m	C_{trace_FPC}	3.6 pF/m
C_{GND_PCB}	71.8 pF/m	C_{GND_FPC}	28.2 pF/m
h_{PCB}	0.0124	h_{FPC}	0.1132

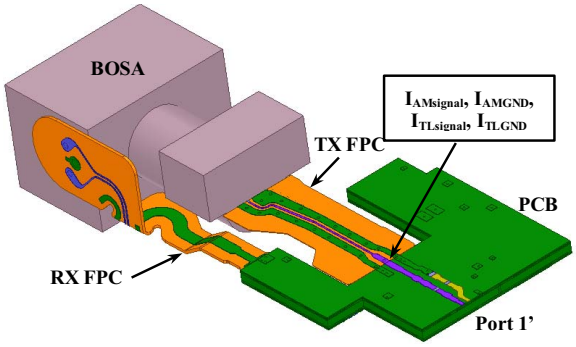

Fig. 6. Illustration of the simplified full wave model of the entire optical QSFP transceiver module under study.

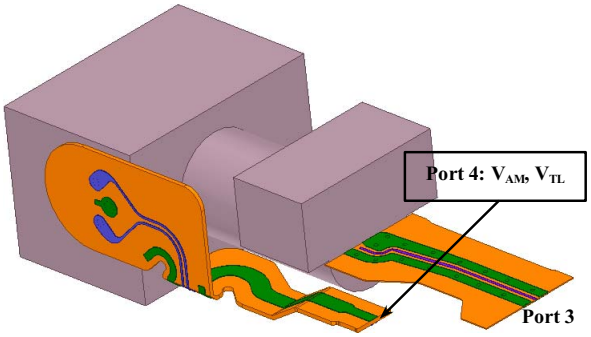

Fig. 7. Illustration of the full wave model with the PCB excluded.

In the full wave simulations, currents can be obtained at various locations using

$$I = \oint \vec{H} \cdot d\vec{l} \tag{2}$$

Electric potential difference can be calculated by doing the integral

$$V = -\int \vec{E} \cdot d\vec{r} \tag{3}$$

The currents flowing on the TX FPC have the following relationship according to their definitions

$$\begin{cases} I_{AMsignal} + I_{AMGND} = I_{AMtotal} \\ I_{AMsignal} + I_{TLsignal} = I_{totalsignal} \\ I_{AMGND} + I_{TLGND} = I_{totalGND} \\ I_{TLsignal} = I_{TLGND} \end{cases} \tag{4}$$

where $I_{AMsignal}$ and I_{AMGND} are the AM currents through the signal trace and reference plane of the TX FPC, respectively. $I_{TLsignal}$ and I_{TLGND} are the useful signal currents propagating on the signal and reference conductors, respectively. Thus, $I_{totalsignal}$ is the total current flowing on the signal conductor and $I_{totalGND}$ is the total currents on the reference plane.

Since $I_{totalsignal}$, $I_{totalGND}$ and the total AM current $I_{AMtotal}$ can be calculated based on (2) assuming differential-mode excitation on the TX traces at port 1' in the simulation model illustrated in Fig. 6, the components of both AM and transmission-line mode excitations at the interface of the PCB and TX FPC, which are $I_{AMsignal}$, I_{AMGND}, $I_{TLsignal}$, and I_{TLGND}, can be obtained by solving (4), allowing the ability to get the induced AM voltage V_{AM} and the coupled voltage V_{TL} when assuming AM and transmission-line mode excitation at port 3 in the simulation model demonstrated in Fig. 7. These voltages are defined as the electric potential differences between the signal and reference conductors at port 4 which is the interface between the PCB and RX FPC.

Table III summarizes the magnitudes of the parameters in Fig. 6 and Fig. 7 at the fundamental frequency. The impact of the AM currents on the total induced noise level at the receiver end is found through the comparison of the magnitudes of V_{AM} and V_{TL} in Table III. The contribution of the EMI noise to the receiver sensitivity degradation is noticeable since V_{AM} and V_{TL} are comparable in magnitude.

V. Mitigation Methods and Experimental Validation

As the AM current on the TX FPC is converted from the CM current on the PCB due to the difference in the imbalance factors, a CM choke manufactured by Murata with part number DLW21SN900HQ2 is applied on the TX channel between the 100 nF AC capacitors and 50 ohm termination resistor to suppress the CM current resulted from the imbalances in the PCB traces.

The CM voltage on the RX channel is measured with and without the application of the CM choke. The CM noise measurement is first conducted in the time-domain using an oscilloscope, and then the waveforms are converted to frequency-domain spectra through discrete Fourier transform [25]. The measurements were performed by using Agilent DSA-X96204Q oscilloscope and N2803A 30 GHz InfiniiMax III Series probe amplifier. One pre-amplifier, Mini-circuit ZVA-443HGX+, was utilized to improve the signal-to-noise ratio of the measurement. The time length and sampling rate of the oscilloscope were set to be 800 ns and 25 GS/s, respectively, based on the 5 GHz fundamental frequency decided by the data rate.

Fig. 8 reveals the effect of the CM choke by comparing the peak envelopes of the measured CM noise on the receiver channel in the frequency domain. The noise level at 5 GHz reduces 7 dB and the eye diagram on the RX channel meets the requirements specified by the manufacturer of the DUT.

Another possible mitigation method is the optimization of the cross-sectional geometries of the PCB transmission line and FPCs with simultaneously considerations on both crosstalk noise suppression and achievement in the least difference in the imbalance factors despite that the CM choke is proved to be effective in the receiver sensitivity improvement. In general, the former is considered to be more cost-effective than the latter especially for massive production. This method is under development and will be reported in the future.

TABLE III. Magnitudes of the Parameters in Fig. 7

Para.	Magnitude	Para.	Magnitude
$I_{AMsignal}$	6.4 mA	V_{AM}	3.3 mV
I_{AMGND}	4.8 mA	V_{TL}	3.8 mV
$I_{TLsignal}$	14.5 mA	/	/
I_{TLGND}	14.5 mA	/	/

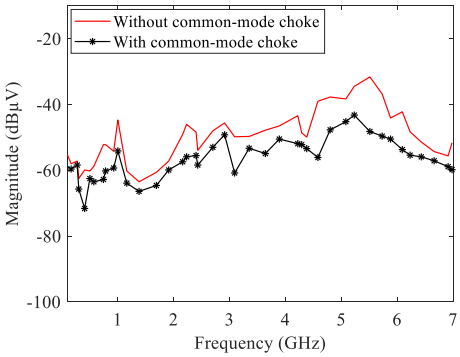

Fig. 8. Comparison of the peak envelopes of the measured CM noise on the RX channel in the frequency domain with and without the CM choke.

VI. Conclusion

In this paper, the receiver sensitivity problem of a typical QSFP transceiver module is studied. The impact of the EMI noise due to the AM current on the receiver sensitivity degradation is demonstrated for the first time. It is shown that the imbalances on the TX channel result in the CM current and the difference in the imbalance factors of the transmission lines on both PCB and TX FPC is the root cause of the generation of the AM current. The effect of the AM current on the unwanted noise at the receiver side is described quantitatively and qualitatively in the full wave simulations. The mitigation method of adding the CM choke is proposed and verified through measurements.

This paper could be helpful for the hardware engineers who design high-speed interconnects or products similar to the optical QSFP transceiver module presented in this paper and the receiver sensitivity is one of the main concerns. The most important lesson learnt from the study is that engineers must pay the same amount of attention to the EMI design as they do in the SI optimization for the products because the unintended EMI noise could fail the DUT and lead to delay in the market release.

Acknowledgment

The authors would like to thank Xinglin Sun for his contributions during his visit at Missouri University of Science and Technology.

References

[1] C. Li, T. Li, G. Guelbenzu, B. Smalbrugge, R. Stabile, and O. Raz, "Chip scale 12-channel 10 Gb/s optical transmitter and receiver subassemblies based on wet etched silicon interposer," Journal of Lightwave Technology, vol. 35, no. 15, pp. 3229-3236, Aug. 2017.

[2] N. Chujo, T. Takemoto, F. Yuki, and H. Yamashita "High-frequency circuit design for 25 Gb/s×4 optical transceiver," 2013 18th Asia and South Pacific Design Automation Conference (ASP-DAC), Yokohama, Japan, Jan. 22-25, 2013.

[3] R. Ammendola, A. Biagioni, G. Chiodi, O. Frezza, F. L. Cicero, A. Lonardo, R. Lunadei, P. Paolucci, D. Rossetti, A. Salamon, G. Salina, F. Simula, L. Tosoratto, and P. Vicini "High speed data transfer with FPGAs and QSFP+ modules," IEEE Nuclear Science Symposium & Medical Imaging Conference, Knoxville, TN, USA, Oct. 30-Nov. 6, 2010.

[4] P. Ma, F. Liu, M. Zhao, H. He, J. Wei, and L. Gao, "Signal integrity design for QSFP interface applicated in RF optical transmitter module," 2018 19th International Conference on Electronic Packaging Technology (ICEPT), Shanghai, China, Aug. 8-11, 2018.

[5] H. Nasu, "Short-reach optical interconnects employing high-density parallel-optical modules," IEEE Journal of Selected Topics in Quantum Electronics, vol. 16, no. 5, pp. 1337-1346, Sep.-Oct. 2010.

[6] W. Gao, Z. Li, J. Song, X. Zhang, F. Chen, F. Liu, Y. Zhou, J. Li, H. Xiang, J. Zhou, S. Liu, Y. Wang, Q. Wang, B. Li, Z. Shi, L. Cao, and L. Wan, "An electrical design and fabrication of a 12-channel optical transceiver with SiP packaging technology," 2010 Proceedings 60th Electronic Components and Technology Conference (ECTC), Las Vegas, NV, USA, Jun. 1-4, 2010.

[7] T. Hino, R. Kuribayashi, Y. Hashimoto, T. Sugimoto, J. Ushioda, J. Sasaki, I. Ogura, I. Hatakeyama, and K. Kurata, "A 10 Gbps×12 channel pluggable optical transceiver for high-speed interconnections," 2008 58th Electronic Components and Technology Conference, Lake Buena Vista, FL, USA, May 27-30, 2008.

[8] X. Jin, K. D. Lystad, and M. H. Sendaula, "Electromagnetic crosstalk penalty in serial fiber optic modules," ICMMT 4th International Conference on Microwave and Millimeter Wave Technology Proceedings, Nanjing, China, Aug. 18-21, 2004.

[9] X. Jin, F. Wang, K. D. Lystad, and M. H. Sendaula, "Electromagnetic crosstalk penalty in 2.5 GB/s and 10 GB/s serial optical modules," 2006 7th International Symposium on Antennas, Propagation & EM Theory, Guilin, China, Oct. 26-29, 2006.

[10] S. Kaneko, T. Saito, A. Sawai, T. Hatta, and K. Kasahara, "Low-crosstalk hybrid-integrated optical transceiver module using a polymer PLC chip and a MMF stub," IEEE Photonics Technology Letters, vol. 13, no. 8, pp. 866-868, Aug. 2001.

[11] I. A. Ukaegbu, M. H. Cho, T. W. Lee, and H. H. Park, "Crosstalk analysis of planar and multi-chip transmitter modules for optical PCB applications," Digest of the 9th International Conference on Optical Internet (COIN 2010), Jeju, South Korea, Jul. 11-14, 2010.

[12] N. Cujo, G. Shinkai, Y. Matsuoka, H. Yamashita, and M. Yasunaga, "Crosstalk reduction for compact optical transceiver module," 2014 IEEE Electrical Design of Advanced Packaging & Systems Symposium (EDAPS), Bangalore, India, Dec. 14-16, 2014.

[13] S. Kim, Y. S. Eom, B. S. Choi, K. S. Choi, H. G. Yun, J. H. Lee, J. H. Park, J. D. Kim, and J. T. Moon, "Electrical crosstalk analysis for gigabit optical transceiver module," CLEO/Pacific Rim 2003. The 5th Pacific Rim Conference on Lasers and Electro-Optics (IEEE Cat. No. 03TH8671), Taipei, Taiwan, Dec. 15-19, 2003.

[14] S. H. Park, and C. S. Park, "Crosstalk improved three channel receiver module for 10 Gb/s parallel optical interconnect application," IEEE MTT-S International Microwave Symposium Digest, Long Beach, CA, USA, Jun. 17, 2005.

[15] S. H. Park, S. M. Park, H. H. Park, and C. S. Park, "Low-crosstalk 10-Gb/s flip-chip array module for parallel optical interconnects," IEEE Photonics Technology Letters, vol. 17, no. 7, pp. 1516-1518, Jun. 2005.

[16] S. Yong, K. Cai, B. Sen, J. Fan, V. Khilkevich, and C. Sui, "A comprehensive and practical way to look at crosstalk for transmission lines with mismatched terminals," 2018 IEEE Symposium on Electromagnetic Compatibility, Signal Integrity and Power Integrity (EMC, SI & PI), Long Beach, CA, USA, 30 Jul.-3 Aug., 2018.

[17] H. Oomori, M. Shiozaki, and H. Kurashima, "Development of a practical electro-magnetic interference (EMI) simulation in high speed optical transceivers," 2009 59th Electronic Components and Technology Conference, San Diego, CA, USA, May 26-29, 2009.

[18] J. Li, X. Li, X. Jiao, S. Toor, L. Zhang, A. Bhobe, J. L. Drewniak, and D. J. Pommerenke, "EMI coupling paths in silicon optical sub-assembly package," 2016 IEEE International Symposium on Electromagnetic Compatibility (EMC), Ottawa, ON, Canada, Jul. 25-29, 2016.

[19] L. Zhang, X. Li, X. Jiao, J. Li, S. S. Toor, A. U. Bhobe, D. J. Pommerenke, and J. L. Drewniak, "EMI coupling paths and mitigation in optical transceiver modules," IEEE Transactions on Electromagnetic Compatibility, vol. 59, no. 6, pp. 1848-1855, Dec. 2017.

[20] T. Wu, W. Jou, S. G. Dai, and W. Cheng, "Effective electromagnetic shielding of plastic packaging in low-cost optical transceiver modules," Journal of Lightwave Technology, vol. 21, no. 6, pp. 1536-1543, Jul. 2003.

[21] D. Kawase, H. Oomori, M. Shiozaki, and H. Kurashima, "EMI suppression of 10 Gbit/s optical transceiver by using EBG structure," 2011 IEEE International Symposium on Electromagnetic Compatibility, Long Beach, CA, USA, Aug. 14-19, 2011.

[22] L. Niu, and T. H. Hubing, "Rigorous derivation of imbalance difference theory for modeling radiated emission problems," IEEE Transactions on Electromagnetic Compatibility, vol. 57, no. 5, pp. 1021-1026, Oct. 2015.

[23] C. Su, and T. H. Hubing, "Calculating radiated emissions due to I/O line coupling on printed circuit boards using the imbalance difference model," IEEE Transactions on Electromagnetic Compatibility, vol. 54, no. 1, pp. 212-217, Feb. 2012.

[24] C. Su, and T. H. Hubing, "Imbalance difference model for common-mode radiation from printed circuit boards," IEEE Transactions on Electromagnetic Compatibility, vol. 53, no. 1, pp. 150-156, Feb. 2011.

[25] Y. Guo, S. Penugonda, M. Kim, J. Lee, J. Ha, S. Yun, J. Fan, and H. Kim, "Ground bridge effect on reduction of conducted emission from three-phase motor drive system," 2019 International Symposium on Electromagnetic Compatibility - EMC EUROPE, Barcelona, Spain, Sep. 2-6, 2019,